



A roller-skating/walking mode-based amphibious robot



Maoxun Li^a, Shuxiang Guo^{b,c,*}, Hideyuki Hirata^c, Hidenori Ishihara^c

^a Graduate School of Engineering, Kagawa University, 2217-20 Hayashichou, Kagawa, Japan

^b Key Laboratory of Convergence Medical Engineering System and Healthcare Technology, the Ministry of Industry and Information Technology, School of Life Science, Beijing Institute of Technology, No. 5, Zhongguancun South Street, Haidian District, Beijing 100081, China

^c Faculty of Engineering, Kagawa University, 2217-20 Hayashichou, Kagawa, Japan

ARTICLE INFO

Article history:

Received 19 May 2015

Received in revised form

21 June 2016

Accepted 29 June 2016

Keywords:

Amphibious robot

Roller-skating mode

Braking mechanism

Modified walking gait

Closed-loop control method

ABSTRACT

An amphibious spherical robot capable of motion on land as well as underwater is developed to implement the complicated underwater operations in our previous research. In order to improve the speed performance of the spherical robot on a slope or comparatively smooth terrains, we propose a new roller-skating mode for the robot by equipping a passive wheel on each leg to implement the roller-skating motion in this paper. A braking mechanism is designed to transform the state of each passive wheel between free rolling and braking states by compressing and releasing the spring, which is controlled by the vertical servo motor on each leg. Besides, in order to improve the walking stability of the wheeled robot in longitudinal direction, a closed-loop control method is presented to control the stability of the direction of movement while walking. Therefore, we conduct the experiments on smooth terrains and down a slope to evaluate the performance of the roller-skating motion, including gait stability and velocity. Finally, plenty of walking experiments are conducted to evaluate the ability of directional control.

© 2016 Elsevier Ltd. All rights reserved.

1. Introduction

As amphibians possessing strong abilities to adaptation in the various environments, a few studies have focused on the amphibious robots inspired by amphibians [1–5,22,23]. In our previous research, we designed and developed a novel amphibious spherical robot with transformable composite propulsion mechanisms, as shown in Fig. 1 [6]. The composite mechanism is designed to switch between water-jet propeller and leg. Using the leg mode, the amphibious robot is able to move from the water to the ground without manpower, and vice versa. However, there are some limitations on the movement speed and the gait stability on land.

As we know, walking robots on land including biped robots, quadruped robots and multi-legged robots, can select discrete foot placement with multi-articulated legs, which causes the robot to have a high efficiency and stability even on rugged terrains [7–9]. With the advantages of having the adaptive capacity to complicated terrains and higher energy efficiency on deformable terrains, researches of the walking robots have been focused on by researchers around the world and some robots edge closer to practical use. Locomotion, as one of the basic functions of a mobile robot, becomes an important indicator of performance evaluation

of the robot, including the movement speed and the ability of directional control. For a walking robot, it can implement a holonomic and omnidirectional motion and can move on soft terrains. Besides, it can also be a stable and movable platform for a manipulator when it stops walking.

However, on the hard level terrain, wheeled locomotion shows a better performance than legged locomotion in terms of mobile velocity and energy efficiency, especially on a slope. When the wheeled robots stop providing the motive power, they are in passive motion with free rotation of the wheels, which can decrease the energy consumption. Consequently, many researches proposed the combination of the advantages of the locomotion of the legged robots and wheeled robots through leg-wheel hybrid vehicles.

In the previous researches, some of the hybrid vehicles are equipped with driven wheels, while others are outfitted with passive wheels. Compared to active wheel-legged robots, passive wheel-legged robots have the advantages of low energy consumption and low weight and compact structure, because driving the active wheels requires actuators, which are usually heavy and bulky. Since the robot in walking mode is already heavy enough, equipping driven wheels will cause in a serious defect during walking.

As the early leg-wheel hybrid mobile robots, the passive wheel-legged robot named Roller-Walker with two actuating modes is proposed [10–13]. The quadruped robot has one passive wheel on each leg, which can be transformed into sole mode by rotating the

* Corresponding author at: Faculty of Engineering, Kagawa University, 2217-20 Hayashichou, Kagawa, Japan.

E-mail address: guo@eng.kagawa-u.ac.jp (S. Guo).

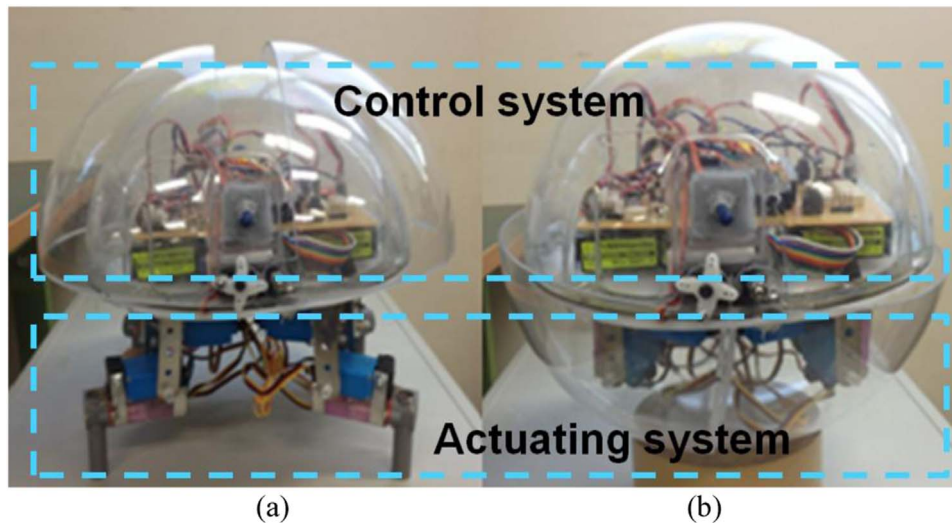


Fig. 1. The amphibious robot in (a) quadruped walking mode, and (b) water-jet propulsion mode.

ankle roll joint. With this transformation mechanism, the locomotion can be switched from quadruped walking to roller-skating on the flat ground. Each leg has three degrees of freedom, one of which is just used for the transformation of the actuation modes. Body extendable quadruped robot (BEQR) is a novel wheel-legged robot with extendable body [14]. Each leg is equipped with a passive wheel and has four degrees of freedom. These two kinds of robots are actuated by passive wheels while roller-skating. Another leg-wheel hybrid platform named Quattroped is designed, which has two separate mechanisms, wheels and legs [15]. With a leg-wheel switching mechanism, the robot can implement the locomotion switching from the wheel mode to the leg mode by shifting the hip point out of the center of the rim. And a leg-track-wheel articulation-based robotic platform, AZIMUT, possessing abilities of adaptation to three-dimensional environments, is developed [16]. However, these two kinds of active wheel-legged robots are heavy and bulky because active wheels need to be driven by additional motors. And all the robots should consider their ability of directional control during walking.

For our previous amphibious robot, the maximum walking velocity on the even terrains, especially on a slope, is not enough for the movement on land. Moreover, the robot can only walk down a slope with a maximum inclination angle of 8° . Additionally, the vibration in yaw direction is generated while walking due to the roughness of the ground. Because of the torus contact surface between the robot leg and ground, it is easy for the robot leg to stumble over the bulges on the ground, which causes the moving direction unstable.

Therefore, in order to improve the on-land performance of the robot, we proposed a new roller-skating mode to improve the on-land speed performance of the robot on the smooth flat surface as well as down a slope. Considering the compact structure of our robot, it was equipped with passive wheels. A braking mechanism was designed to implement the transformation of state of each passive wheel between free rolling state and braking state by controlling the vertical servo motor to compress and release the spring. Using a transformation mechanism, a modified walking gait was applied to the robot to implement the walking motion in the meantime. Besides, we developed a closed-loop control algorithm to realize the directional control of the robot during walking. Roller-skating experiments are conducted to evaluate the performance of sliding motion, and walking experiments of the robot in modified walking gait are also carried out. Finally, the walking experiments of the robot with the closed-loop control system are

conducted to evaluate the performance of directional control.

The remainder of this paper is organized as follows. In Section 2, we describe the general design of the previous amphibious spherical quadruped robot. In Section 3, we introduce the new structure of the robot in roller-skating mode, actuating mechanism for movement, a novel roller-skating gait and the control system. The braking mechanism and transformation mechanism are described, and a modified walking gait is presented in Section 4. The development of a prototype in roller-skating/walking mode is described, and results of on-land experiments in these two modes are presented in Section 5. Section 6 introduces a closed-loop control method for directional control of the robot and plenty of closed-loop control experiments. Section 7 concludes the paper.

2. General design of our previous amphibious robot

In our previous research, we developed an amphibious spherical robot capable of motion on land and underwater to perform complicated operations [6]. The configuration and physical dimensions of the amphibious spherical robot are illustrated in Fig. 2. To obtain a better performance in terms of adaptation to various complex environments, on land and underwater, the spherical robot can change its actuating mode between water-jet propulsion mode [21] and quadruped walking mode with transformable composite propulsion mechanisms. The amphibious robot is able to move from the water to the ground without manpower, and vice versa.

The amphibious robot is composed of a sealed transparent upper hemispheroid, two openable transparent quarter spherical shells, a plastic circular plate and four actuating units, each of which consists of a water-jet propeller and two servo motors, as shown in Fig. 2. With the two mutually perpendicular servo motors fastened to the same actuating unit, each actuating unit can realize two degrees of freedom movement. The control circuits, batteries and sensors are carried on the sealed hemispheroid for being waterproof. The diameter of the upper and lower hemisphere is 234 mm and 250 mm respectively. The height of the actuating unit in standing state is 108 mm.

From the results of our previous researches [17,18], the maximum walking velocity of the robot on the even terrains is 22.5 cm/s, which is not enough for the on-land movement especially moving down a slope. Besides, the robot cannot climb a ramp over an inclination angle of 8° as a result of its higher center

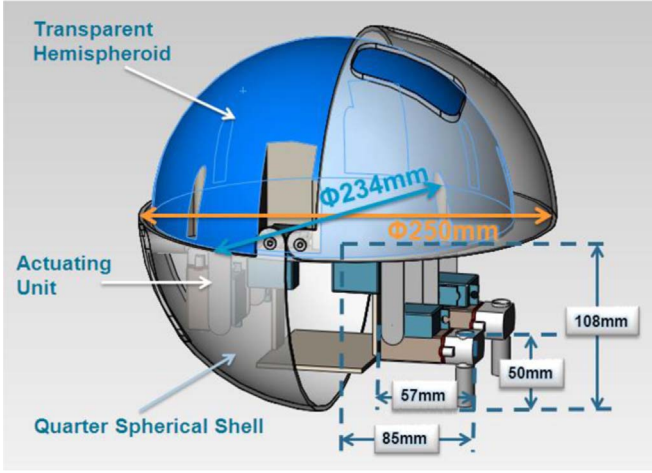


Fig. 2. Physical dimensions of the amphibious spherical robot.

of gravity. During the walking motion, the robot lifts four legs one by one or the two of them at one moment, which causes the robot to break its balance due to the shifting of the center of gravity. If the robot slides downhill with passive wheels, the position of center of gravity will not change during this period. The robot can keep the balance and prevent tumbling forward during sliding downhill. Therefore, the contribution of this paper is to propose a roller skating-walking hybrid mode to improve the on-land performance of the robot especially on the smooth flat surface as well as down a slope.

3. Proposed roller-skating mode

Using multi-articulated legs is able to select discrete foot points during quadruped walking motion on land, which produces a high efficiency and stability for the robot even on rugged terrains. On flat terrains and ramp, wheeled locomotion is more efficient than legged motion due to the low friction along the direction of motion [10].

3.1. Design concept of the robot in roller-skating mode

To increase the adaptability to different terrains and improve the mobile velocity of the quadruped robot on level or comparatively smooth terrains and ramp, each leg installs a passive wheel on it to implement roller-skating motion without an additional motor, which increases an on-land hybrid mechanism for the robot with light weight, as shown in Fig. 3. Each wheel has one passive degree of freedom and is fastened to the lower surface of the motor of water-jet propeller next to the nozzle. The lateral surface of each wheel is facing to the central axis of the robot in standing state. The wheel is made of rubber and can rotate around the axis with lower friction. Because the height of the wheel component is larger than that of the nozzle component which used to be the leg to support the robot, wheel becomes the new support connected to the ground.

With this new structure, a transformation mechanism is required for the robot to switch the locomotion between roller-skating and quadruped walking to implement the two kinds of motions. Consequently, a brake apparatus is designed and used not only as a braking mechanism but also as a transformation mechanism between two actuating modes, with which the passive wheel can be transformed from free rolling state into braking state by releasing the spring to prevent the wheel rotating. Legs with passive wheels have three degrees of freedom, including two

active degrees of freedom actuated by the two servo motors and one passive degree of freedom around the axis of the wheel. The new actuating system of the improved robot is shown in Fig. 4. The direction of motion while walking is the same as that during roller-skating.

3.2. Gait characterization and kinematic model

Roller-skating uses wheels initially to provide pushing force by exploiting high lateral ground reaction forces and subsequently to reduce friction along the direction of motion, which allows the subject to slide forward. In the moving range of legs, there are a large number of possible trajectories. In a classic roller-skating motion, the human skater pushes one leg out and then makes it get full extension. In this process, the other leg is used as a supporter with its passive wheel freely rotating until the skater recovers the preceding extended leg to its starting position. The two legs drive the skater alternately and each leg pushes off the ground consistently in one direction (e.g. the right leg only moves to the right) [19].

A roller-skating gait proposed for the quadruped robot is inspired by the classic roller skating motion of human being. In the initial state of the skating motion, all the legs should keep vertical to the ground and should be aligned with the direction of motion of the robot. In the skating process, two front legs remain in contact with the ground at all times with the horizontal and vertical servo motors fixed at a constant angle and keep the rolling surface of each wheel facing forward; two rear legs implement the pushing movement periodic alternately. When one rear leg is actuated to push the ground, the rotational angle of the two servo motors of the other rear leg is fixed and the leg keeps its wheel's rolling surface facing forward as the front legs. For the sliding forward motion, two rear legs are controlled by the robot to implement an alternately cyclical motion with at least three wheels facing forward at any one time, which indicates that the robot's center of gravity must remain inside a polygon formed by the supporting legs.

With roller-skating gait, the front legs only have one phase, the free rolling phase; while the rear legs have three phases, including the free rolling, sliding and propulsion phases. In the free rolling phase, the leg remains stationary and the passive wheel rotates freely around the axle which is fixed at a right angle to the leg. In the sliding phase, the horizontal servo motor of the rear leg will rotate 60° anti-clockwise, while the vertical motor will rotate 20° anti-clockwise. During this period, due to the low friction generated by the rolling motion of the wheel, the friction resistance can be overlooked or ignored. In the propulsion phase, the rotational angle of the horizontal motor remains the same as the final state in the sliding phase and the vertical motor will rotate 40° clockwise to produce driving force for the robot, as shown in Fig. 5. Assuming that there is no slip in the propulsion phase, the friction force formed by relative motion between the moving wheel and the ground, as the driving force of the robot in roller-skating mode, can be expressed as follows:

$$f(t) = F_2(t) = F \cdot \cos\theta(t) = \frac{T}{h} \cdot \cos\theta(t) \quad (1)$$

$$F_r(t) = f(t) = \frac{T}{h} \cdot \cos\theta(t) \quad (2)$$

where $f(t)$ is the friction force generated by the vertical servo motor, T is the rated torque of the servo motor, h is the moment arm, $F_r(t)$ is the driving force of the robot, $\theta(t)$ is the amplitude of the swing angle around the axis of vertical servo motor, θ_m is the maximum amplitude, and μ is the friction coefficient between the

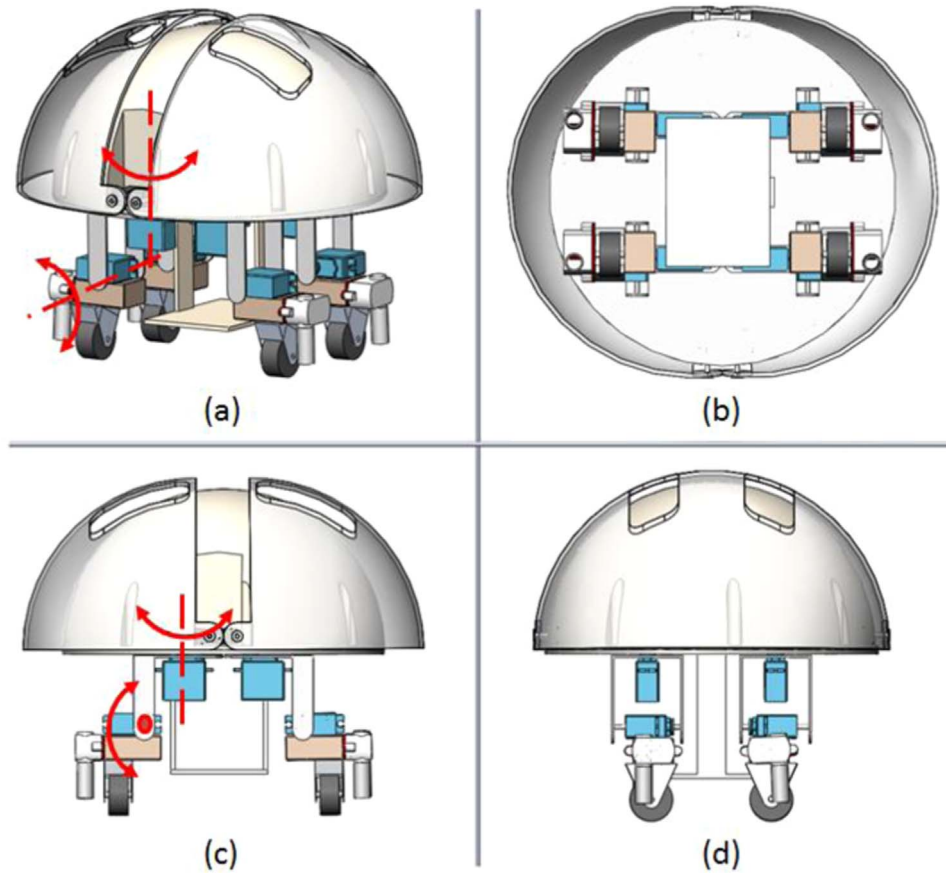


Fig. 3. Structure of the robot in three actuating modes: (a) overall structure, (b) bottom view, (c) front view and (d) side view.

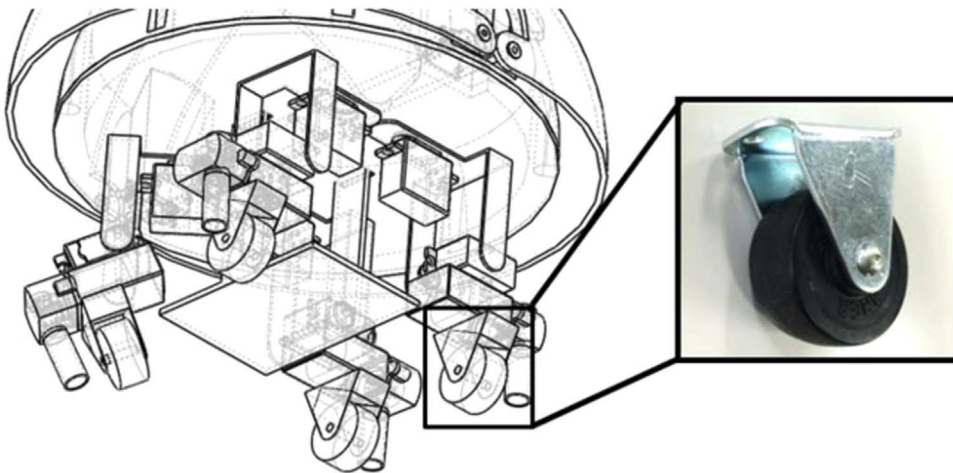


Fig. 4. New actuating system with three actuating modes.

wheel and ground.

The resultant force F_r is the driving force while roller-skating. However, the resultant force acting along the ground plane can be summarized as the longitudinal force to actuate the robot to slide forward and the transversal force to generate a lateral displacement as shown in Fig. 6. Due to the presence of the transversal force, the robot will not go straight exactly. The force imposed by the left rear leg is the same with that formed by the right rear leg at any position. Consequently, the robot will move along a wave trajectory, as shown in Fig. 7(a). The wave trajectory can be fixed by the amplitude and frequency of the swing motion of each rear leg. Due to the symmetry, the transversal reaction force generated

by the two rear legs can be counteracted after finished one-cycle sliding motion. Therefore, the robot will move to a destination right ahead. The longitudinal force and the transversal force can be obtained as follows:

$$F_{r1}(t) = F_r(t) \cdot \sin\alpha(t) \quad (3)$$

$$F_{r2}(t) = F_r(t) \cdot \cos\alpha(t) \quad (4)$$

where $F_{r1}(t)$ is the driving force acting parallel to the robot's moving direction, $F_{r2}(t)$ is the driving force acting perpendicularly

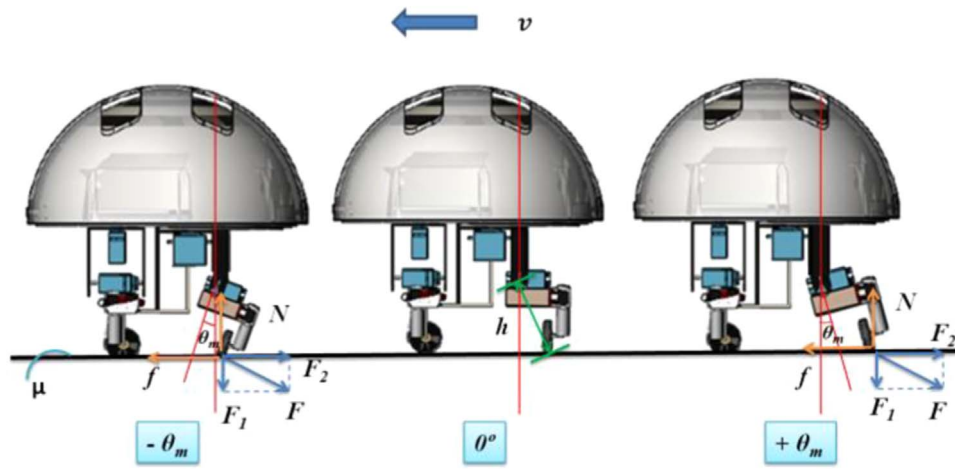


Fig. 5. Force analysis in the propulsion phase (side view). The blue arrows indicate the direction of the force applied on the ground by robot. The orange arrows indicate the direction of the force applied on the wheel of the robot by ground [20].

to the moving direction, α is the maximum amplitude of the swing angle around the axis of horizontal servo motor.

Utilizing alternating movements of two rear legs, the robot can

realize the sliding forward motion with the rolling surfaces of the front wheels facing forward. Since the rear legs can produce an actuating force through pushing off the ground, the robot can

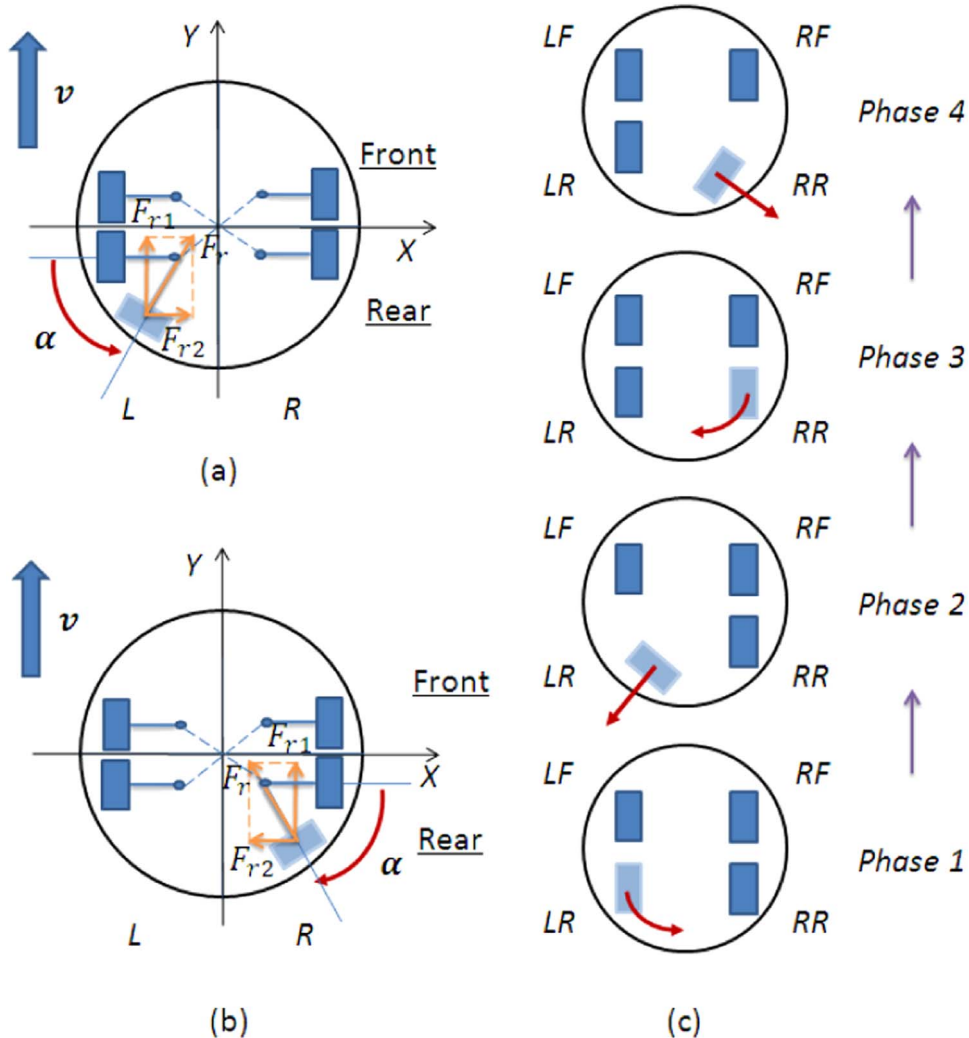


Fig. 6. Ground reactive force analysis on (a) left rear wheel and (b) right rear wheel while roller-skating and (c) gait cycle diagram in sliding and propulsion phases (top view). Phase 1 and 3 are sliding phases; phase 2 and 4 are propulsion phases. The legs are labeled as follows: left fore (LF), right fore (RF), left rear (LR), and right rear (RR). The light blue rectangle indicates the driven leg moving with three degrees of freedom, while the dark blue one indicates the leg moving with passive degree of freedom. The red arrow indicates the direction of movement of the rear wheel.

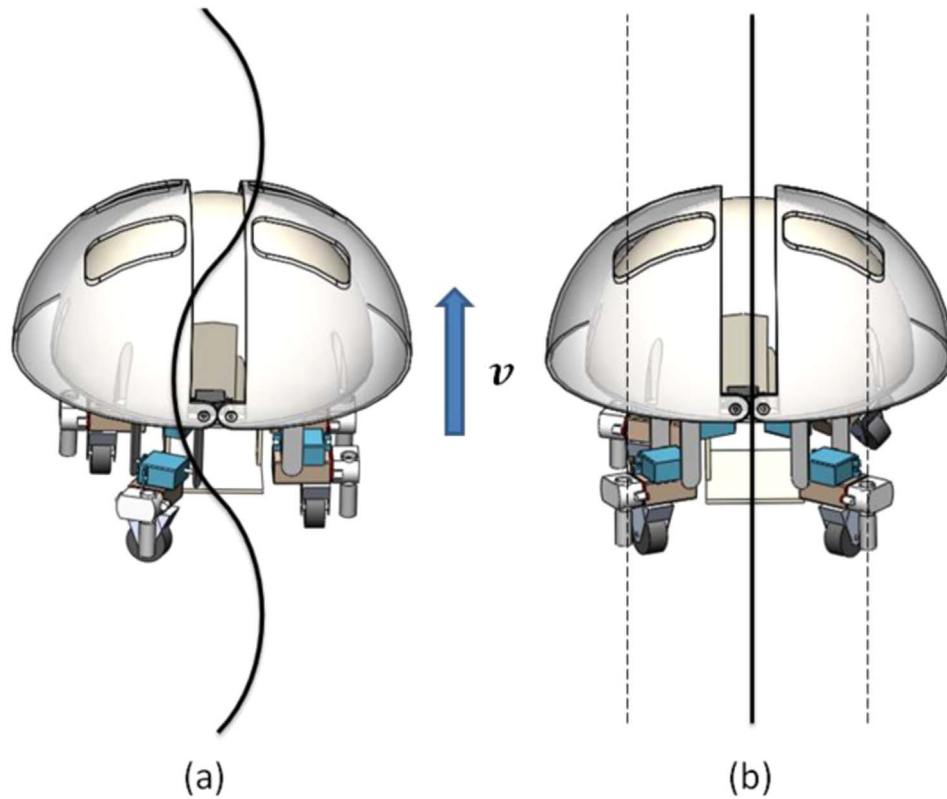


Fig. 7. Leg trajectory when (a) roller-skating and (b) walking.

make turns by steering the front legs. During the turning motion, the horizontal servo motors of the two front legs are controlled to rotate clockwise or anticlockwise to change the turning direction.

3.3. Control system mechanisms and batteries

The control center of the spherical robot is AVR micro-controller. We use ten channels of PWM signals to control the eight servo motors on the legs and two servo motors on the upper hemisphere to open and close two quarter spherical shells. We also use eight Input/output ports to control four water jet propellers for positive rotating and negative rotating motion. Another four Input/output ports are connected to the four channel remote controller which controls the movement of the robot.

For the power supply, we use three batteries, one of which, 6TNH22A/8.4 V, is for providing the power to AVR micro-

controller, other two of which, YBP216BE/7.4 V, are used to provide the power to ten servo motors and four water jet propellers.

4. Modified walking mode and transformation mechanism

4.1. Braking mechanism

As we mentioned in Section 3, two front legs remain their initial positions at any time while sliding and two rear legs perform the pushing movements alternately. In a classic braking motion for roller-skating, the human skaters drag the toe stop along the ground to produce a resistance along the direction of motion or change their pose to a pigeon-toed pose to slow down. Since a human ankle has three active degrees of freedom, human can realize these two braking motions quickly and easily. However, it is

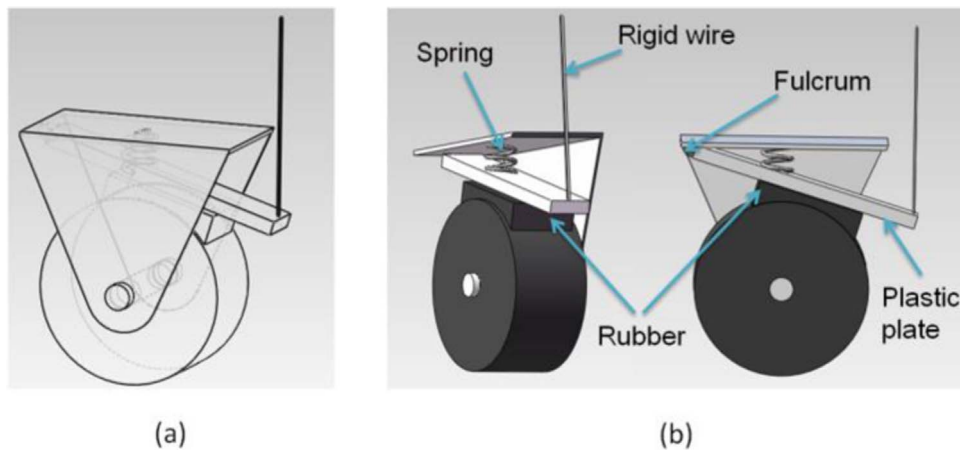


Fig. 8. Braking mechanism of the wheel: (a) overall structure and (b) cross-section diagram.

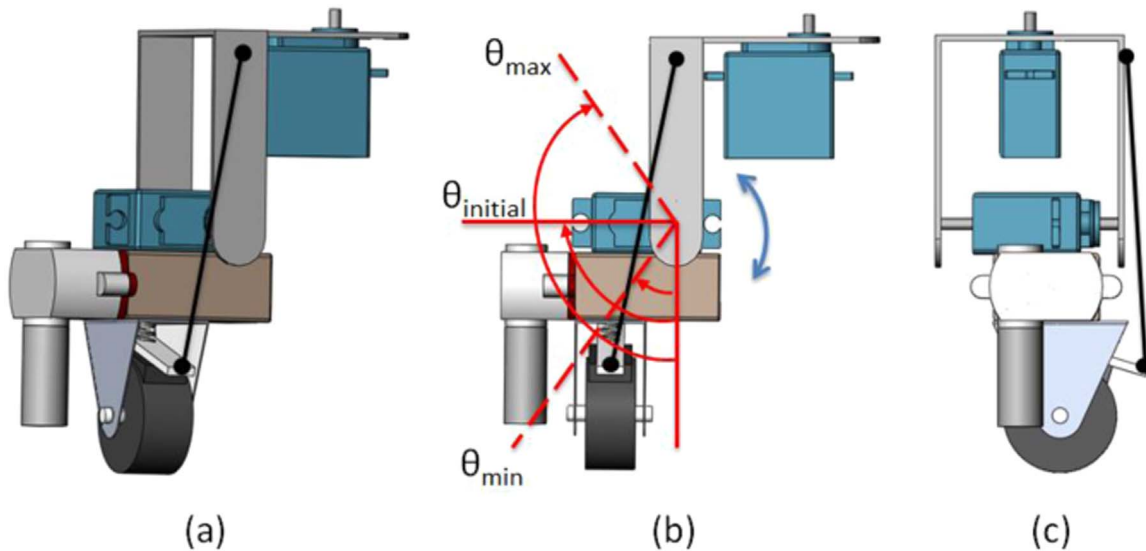


Fig. 9. Leg-wheel hybrid actuation system: (a) overall structure, (b) front view and (c) side view.

difficult for the quadruped robot to stop with these two methods due to the wheel part only having one passive degree of freedom. Therefore, a braking mechanism is required to stop the robot instead of the traditional ways.

Adding braking equipment for each leg will cause serious weight increment and volume increases on the robot. Since the robot has a compact structure and actual torque of servo motor is limited according to the rated torque, additional braking equipment should not be carried on the robot's legs. Accordingly, a novel braking mechanism of wheel is proposed to implement the braking motion, as shown in Fig. 8. Using this mechanism, no more additional devices are needed for braking motion. By changing the rotational angle of the vertical servo motor, the robot can apply brake and loose brake.

Fig. 8(b) shows the proposed braking equipment, which is composed of a fulcrum, a spring, a plastic plate, a rigid wire and a rubber. The rough rubber is used as a brake pad to be squeezed against the wheel. The rigid wire linked to the end of the plate is connected to the vertical motor bracket, as shown in Fig. 9(a). When the rigid wire is in a tight state, the spring is compressed to separate the rubber from the wheel, which implements a free rolling for the passive wheel. When the rigid wire is in a loose state, the compressed spring will apply an elastic force on the rubber to make the rubber contact with the wheel completely, which makes the actuation unit be a leg while walking.

4.2. Transformation mechanism

In order to implement the walking and roller-skating motions for the robot in the new structure at the meantime, a transformation mechanism, which can switch the robot's locomotion between roller-skating and quadruped walking, is required. As rotating the vertical servo motor can tense and loose the rigid wire to change the state of wheel between free rolling and braking states, the proposed braking mechanism can also be used as a transformation mechanism to perform the mode switching between walking and roller-skating modes.

The rotational angle of the vertical motor is in a range of θ_{min} to θ_{max} while walking and roller-skating. The initial angle $\theta_{initial}$ shown in Fig. 9(b) indicates the initial state of the robot's leg when roller-skating. The vertical servo motor in the initial state tenses the rigid wire just right to separate the rubber from the wheel, remaining the wheel in free rolling state. When the motor rotates

anticlockwise from the initial position, the wire will be pulled tighter to loose brake as like in the initial state; when the motor rotates clockwise from the initial position, the wire will be released to apply brake.

We have mentioned that two front legs and one rear leg are in the initial state and the other rear leg implements the sliding and propulsion phases during roller-skating. In the initial state, wheels can roll freely without applying brake. In sliding phase, as the rotational angle of the motor is less than the initial angle, the wheel of active rear leg performs the free rolling motion. Additionally, in the propulsion phase, the wheel rotates around the axis of the vertical motor, which is perpendicular to the axle, to push off the ground to generate the driving force in two directions. In the propulsion phase, the robot will loose brake at first and then apply brake, which has no effect on the movement of the robot.

The rotational angle of the vertical motor in the initial state is 1 degree larger than $\theta_{initial}$ while walking motion. The rotational angle in walking mode is in a range of the walking initial angle to the maximum angle θ_{max} . During the walking motion, all the wheels are in braking state at any time.

4.3. Modified walking gait

Generally, robot utilizes large ground reaction forces to implement walking motion. In our previous research, the nozzle component was used as the leg during the walking motion. To adapt to different environments, quadruped robots with two degrees of freedom in each leg could use three different gaits [6]. For the robot in new structure, since the height of the wheel component is larger than that of the nozzle component, wheel becomes the new support connected to the ground. Moreover, the initial state in previous walking mode is used to be that in roller-skating mode. As the initial angle of vertical motor is changed when walking, the previous walking gait will not apply to the modified robot. However, the previous gait characteristic can be utilized to realize three different walking gaits. From previous results of on-land experiments, the third gait had the best performance while walking and rotation. Hence, the modified robot will employ the gait characteristic of the third gait as that of the modified walking gait. By changing the variation of rotational angle of the vertical motor, we achieved a modified walking gait. The robot can realize the walking and rotating motions with this modified walking gait. From our previous research, we know that the velocity of the robot

in walking mode is related to the step size and frequency of the gait cycle, i.e.,

$$v = d * f \quad (5)$$

where v is the velocity of the robot, d is the step size of the robot, f is the frequency of one step cycle [6]. As there are losses on step size mainly caused by the limited response time of the servomotors at high frequencies, the step size increases in terms of the frequency of the gait cycle at low frequencies, and then decreased towards zero at high frequencies. According to the Eq. (5), there exists a maximum walking velocity as a function of the frequency of the gait cycle.

5. Prototype robot in two land modes and experiments

5.1. Sliding/walking experiments on a smooth flat surface

A prototype quadruped robot with walking, roller-skating and water-jet propulsion modes was developed, as shown in Fig. 10. Four passive wheels are installed on four legs of the robot. And each leg has one passive and two active degrees of freedom. Moreover, a braking mechanism is added to the wheel on each leg to apply brake when required.

In order to evaluate the performance of the robot while roller-skating and walking, both sliding and walking experiments on a smooth flat surface were conducted. With roller-skating gait, the robot used the friction force as the driving force to move along a wave trajectory, as shown in Fig. 11. Although the rear legs cannot provide propulsion when sliding motion stops, the robot can move forward with lower friction between wheel and ground due to the inertia effect. With braking mechanisms, four brake pads are separately controlled to be squeezed against each wheel to reduce the speed of the robot and finally stop the robot. The experimental results of roller-skating motion at different control frequencies are shown in Fig. 12. The curve marked in red shows that the roller-skating velocity initially increased as a function of control frequency, and then decreased. At high frequencies, as the slip between the wheel and the ground becomes serious as a function of the frequency, the sliding velocity decreases. And a maximum roller-skating velocity of 37.8 cm/s was achieved.

With the transformation mechanism, the robot can realize walking and rotating motions with modified walking gait. To evaluate the walking performance, we measured the walking velocity at different frequencies with modified walking gait. In Fig. 12, the curve marked in green indicates the walking velocity. From the results, as the frequency increased, the walking velocity

increased at first, and then decreased to zero. The velocity of the robot is related to the step size and frequency. We achieved a maximum walking velocity of 22 cm/s. At relatively low frequencies, the walking and roller-skating velocities of the robot were approximately equal. It is obvious that at relatively high frequencies the sliding motion shows better performance than the walking motion. Compared to walking motion, sliding motion is not affected by the response time of the servo motor, which had a big influence on walking motion at relatively high frequencies.

Besides, rotating experiments were conducted to evaluate the performance of rotating motion with rotating gait. As shown in Fig. 13, the green curve indicates the results of rotating velocity at different frequencies. The rotating velocity has the same rule change with the walking velocity as a function of frequency with modified walking gait. As we mentioned in our previous research, at low frequencies, the step size increased as a function of the frequency of the gait cycle, and then decreased towards zero at high frequencies [6]. And we achieved a maximum rotating velocity of 66.7°/s.

5.2. Sliding/walking experiments on a slope

To evaluate the slope performance of the robot when walking and sliding, walking and roller-skating experiments were carried out down a slope. On a slope, the component force of gravity of the robot provides part of the driving force, which causes the robot to achieve a relatively high velocity. A crucial aspect of moving down a slope is to maintain balance, which means that the robot's center of gravity must remain inside a polygon formed by the supporting legs. Since the two front legs are in the initial state all the time during sliding, sliding motion will be stable than walking motion. Fig. 14 shows the experimental results of the walking and sliding velocities down a slope at an inclination angle range of 0° to 10°. The curve marked in red shows that as the incline increased, the roller-skating velocity of the robot increased; while the curve marked in green shows that the walking velocity initially increased as a function of incline, and after the inclination angle is over 7° the robot cannot keep balance on the incline. We achieved a maximum roller-skating velocity of 62.1 cm/s. Roller-skating gait showed a better performance than modified walking gait down a slope, allowing the robot to move downhill an inclination of 10°.

6. Closed-loop control of the direction of movement

6.1. Design of the closed-loop control system

Gait stability is a principal element to evaluate the motion of a mobile robot, because precise position control is necessary for operations and all the tasks both on land and underwater need a stable working platform. Attitude information of a robot contains three angles, including pitch, roll and yaw angles. According to the results of the previous gait stability experiments, the vibration of the robot's body in pitch and roll directions during walking and rotation existed and could not be avoided, but it had less influence on the direction of movement of the robot. However, vibration in yaw direction makes a great influence on the robot's locomotion. For the improvement of the walking stability of the wheeled robot in longitudinal direction, a closed-loop control method is designed to control the stability of moving direction during the walking motion.

For the previous robot, because of the torus contact surface between the robot legs and ground, it is easy for the robot legs to stumble over the bulges on the ground, which causes the moving direction unstable. However, for the revised robot with four wheels, the wheels support the robot on the ground instead of the

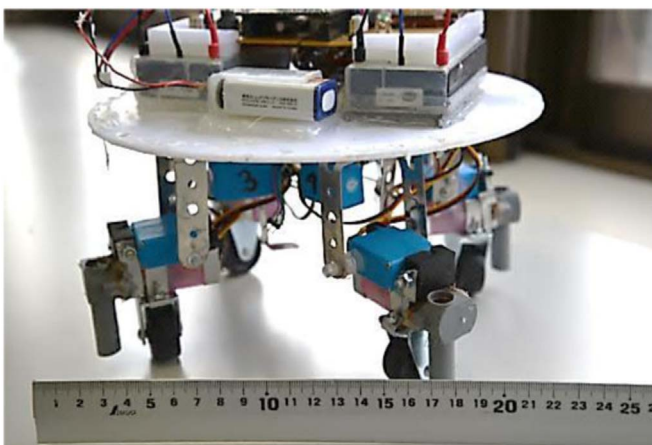


Fig. 10. The prototype robot in walking and roller-skating modes.

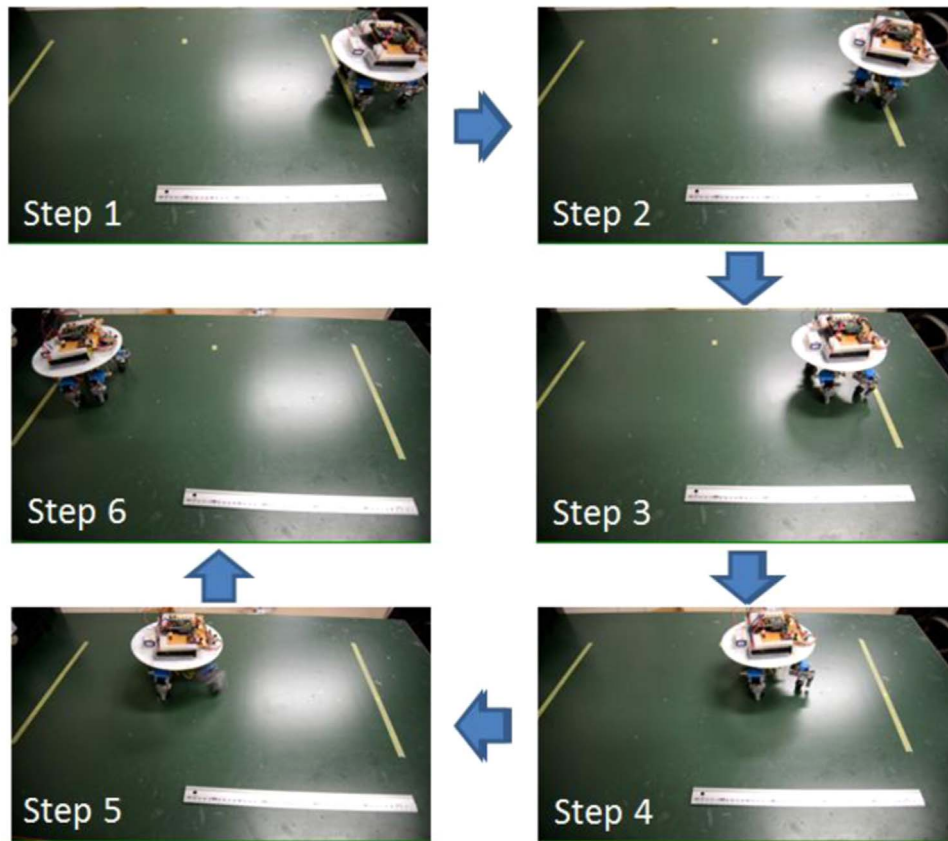


Fig. 11. Experiments with roller-skating gait.

nozzles with the advantages of big contact surface and not easy to stumble. Compared to the previous robot, the revised one shows a better performance on the stability of longitudinal motion. But the robot still has vibration in yaw direction due to the complex ground environments. Therefore, the yaw angle, an attitude angle, must be obtained to realize a closed-loop control on the movement stability. A gyroscope sensor, ADIS16265, was carried on the robot to measure the yaw angle for the control of moving direction. During the walking motion, when a yaw angle measured by

ADIS16265 is over 10° , the robot is set to change its motion from walking to rotation to make its body face forward. According to this setting, the rotational angle of one gait cycle should be over 10° and as close to 10° as possible. Consequently, an appropriate control frequency with the modified walking gait is required to achieve a rotational angle as close to 10° as possible during one gait cycle.

In order to achieve an appropriate rotational angle during one gait cycle, we did the calculation using the gained rotating

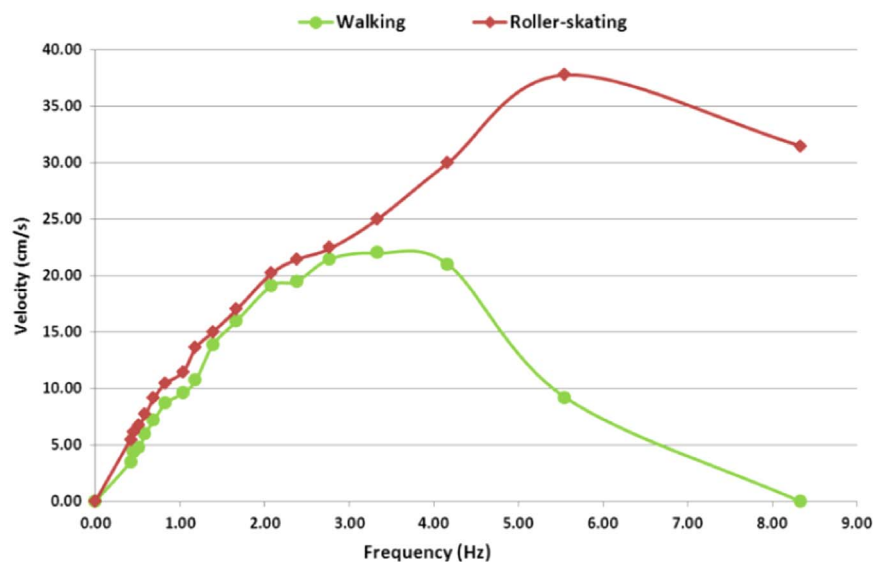


Fig. 12. Experimental results of the robot in roller-skating and walking modes. The control frequency is the movement frequency of the driving leg. The red and blue lines correspond to roller-skating and walking motions respectively.

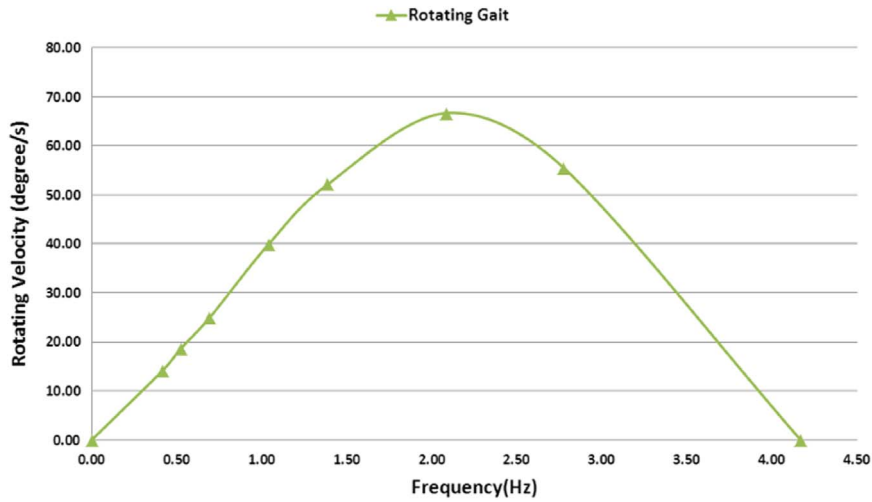


Fig. 13. Experimental results of rotating velocity of the robot with rotating gait.

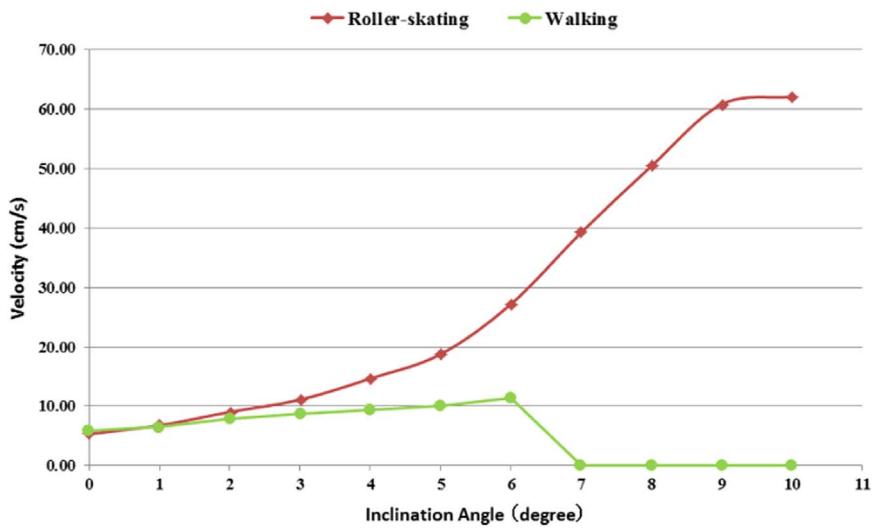


Fig. 14. Experimental results of the robot in roller-skating and walking modes down a slope with different inclination angles.

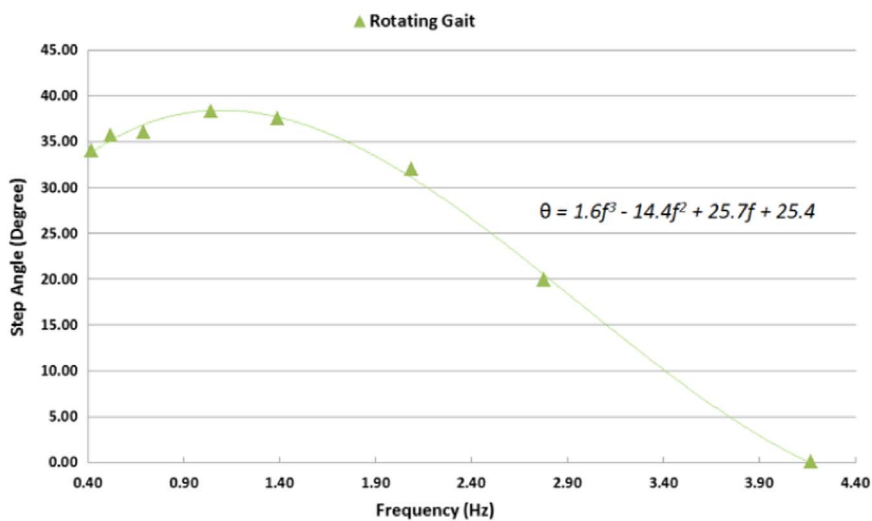


Fig. 15. Experimental results of the step angle of the robot with rotating gait.

velocities in Fig. 13 to get the relationship between step angle and step frequency. The rotating velocity is related to the step angle and step frequency of the gait cycle, i.e.,

$$\omega = \theta * f \tag{6}$$

where ω is the rotating velocity, θ is the step angle of one gait

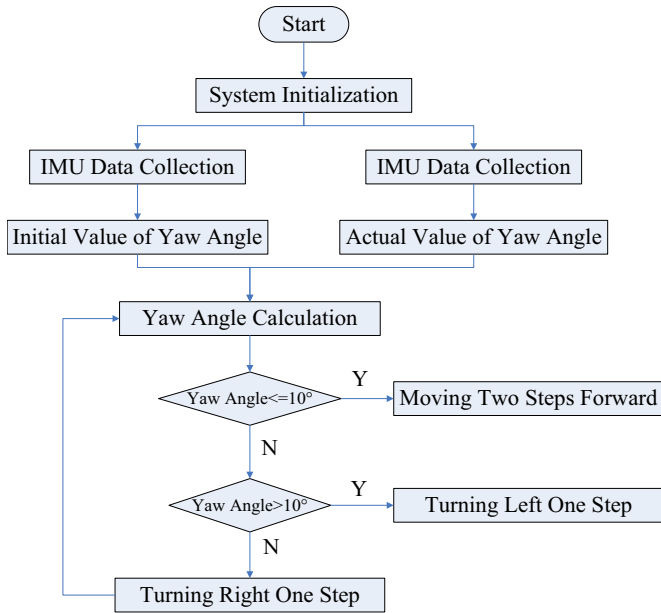


Fig. 16. Flow chart of the longitudinal motion control system.

cycle, f is the control frequency of the gait cycle.

According to the Eq. (6), we achieved the relationship between the step angle and step frequency. As shown in Fig. 15, the green points imply the results of the step angle of one gait cycle as a function of control frequency. From the results, we can see that as the step frequency increases, step angle slightly increases at first, and then decreases to zero. Fig. 15 shows the approximate curve and the equation of the step angle of the robot with the modified rotating gait. Considering the range of the yaw angle, a step rotational angle of 11° at a control frequency of 3.3 Hz is set for the robot.

Fig. 16 shows a flow chart of the control system of longitudinal motion. The gyroscope sensor is applied to measure the yaw angle of the robot. Depending on the degree of yaw angle, the robot implements the locomotion transformation from walking to rotation. When the degree of yaw angle is less than 10° , the robot is controlled to move two steps forward; when the angle is over 10° , the robot is controlled to spin clockwise or anticlockwise for

getting back to the initial direction.

6.2. Performance evaluation of the gyroscope sensor

In order to control the direction of movement, a closed-loop control method is proposed with a gyroscope sensor equipped on the robot. ADIS16265, a yaw rate gyroscope sensor, operated by a single supply in a range of 4.75 V to 5.25 V is used for the motion control of the robot. Four SPI signals of the gyroscope sensor are used to produce data and make it available to a processor.

By calculating the relative error of the data of rotational angle collected from ADIS16265 by PC, we can achieve the accuracy of the sensor. AVR microcontroller communicates with ADIS sensor by SPI (Serial Peripheral Interface) and transmits the ADIS16265 data to PC over UART (Universal Asynchronous Receiver/Transmitter). We use COMDEBUG on the PC to receive data from ADIS sensor. Serial debug terminal settings are as following: 9600 baud rate, 8 data bit, one stop bit, no parity bit. We manually rotated the ADIS sensor by 90° clockwise and recorded the data from COMDEBUG at intervals of 10° . The data at each angle was recorded after 20 s and the experiment at each angle was repeated 10 times to get the average value. Fig. 17 shows the experimental values of the rotational angle of the sensor and the relative error in the measurements. According to the results in the histogram, we achieved a minimum relative error of 0.5%. Although the relative error at a rotational angle of 10° is 13.6%, which seems to be a little large, the angle error between experimental value and theoretical value is approximately 1° . Therefore, the accuracy of the gyroscope sensor is high enough to implement the longitudinal motion control of the robot.

6.3. Closed-loop control experiments

In order to improve the walking stability of the wheeled robot with the modified gait in longitudinal direction, the ADIS sensor is carried on the robot to measure the yaw angle. Additionally, two kinds of closed-loop control experiments are conducted to evaluate the performance of the control of the direction of movement for the robot based on the closed-loop control system. One kind of the experiments is that the robot moves on the uneven ground. During the walking motion, a yaw angle happens to the robot due to the different step loss of the four legs. The other kind of the

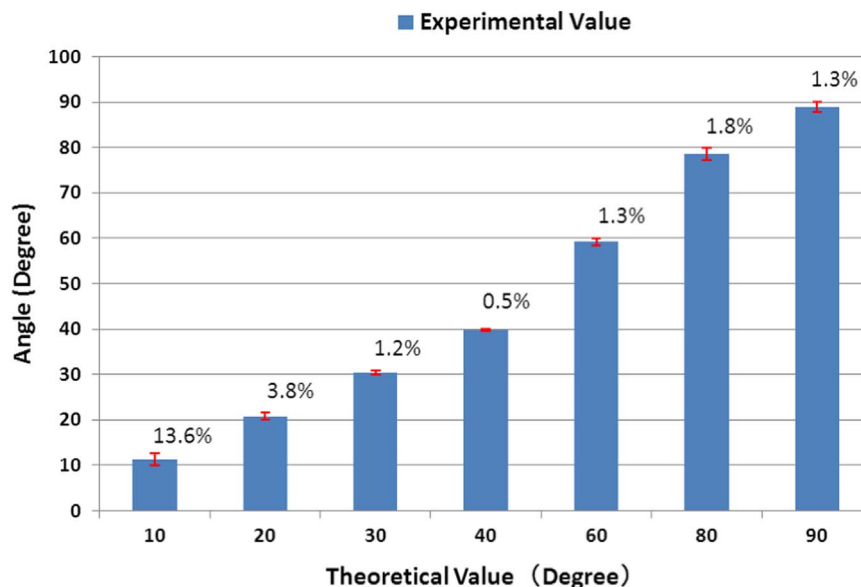


Fig. 17. Experimental values of the rotational angle of sensor and relative error.

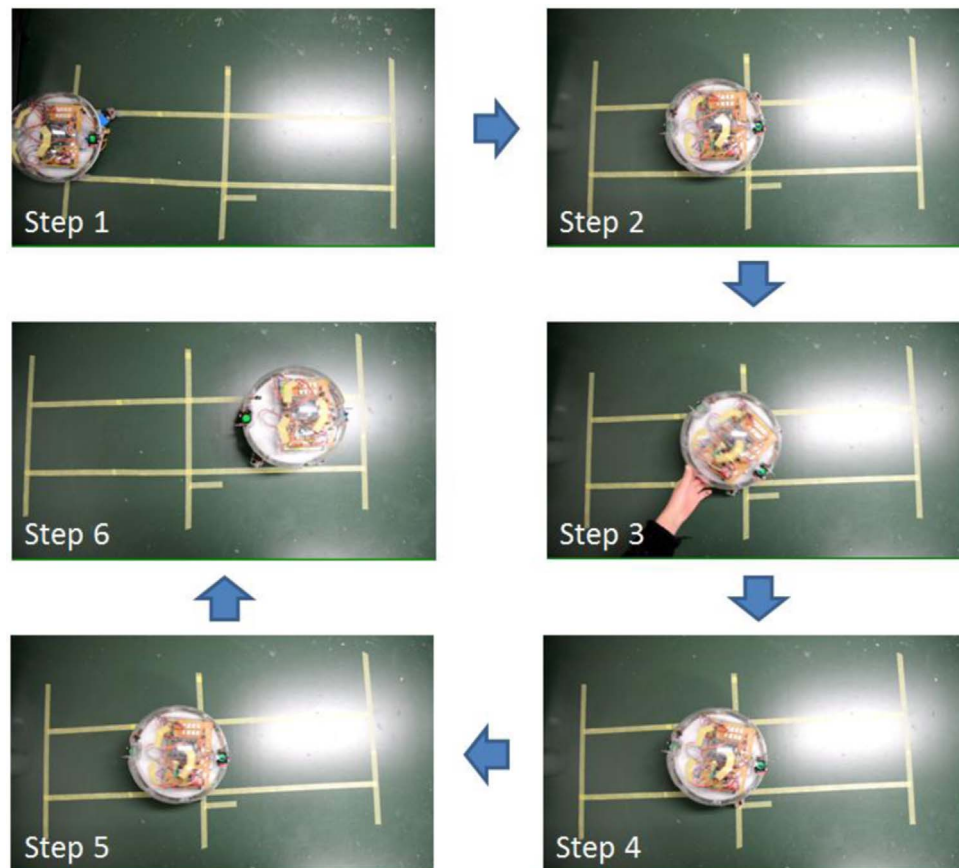


Fig. 18. Closed-loop control experiments of the moving direction of the robot acted upon by an external force.

experiments is that the robot moves on the even ground and an external force is applied on the robot to cause a deviation in the moving direction. Using the closed-loop control system, the moving direction is offset by the rotating motion.

A walking experiment of the robot acted upon by an external force was done for evaluating the ability of the control in longitudinal direction, as shown in Fig. 18. An ADIS gyroscope sensor was employed to measure the change of yaw angle. Through the measurement of the yaw angle in real time, the robot can keep its moving direction by the rotating motion after an external force is applied on it. From the experimental results, the robot performs well in the directional control.

7. Conclusions

For the improvement of the on-land speed performance of the amphibious robot down a slope or comparatively smooth terrains, a passive wheel is equipped on each leg to perform roller-skating motion. We proposed a braking mechanism to realize the transformation of state of each passive wheel between free rolling and braking states by controlling the vertical servo motor to compress and release the spring. The braking mechanism can be used as a transformation mechanism to apply a modified walking gait to the wheeled robot to implement walking motion meantime. Hence, we describe experiments on smooth flat terrains and down a slope to evaluate the performance of roller-skating motion. Additionally, plenty of walking experiments of the robot with modified walking gait are conducted.

At low frequencies, the sliding velocity and walking velocity on the flat terrain were roughly equal. At a control frequency of

5.56 Hz, we got a maximum roller-skating velocity of 37.8 cm/s. And the robot was able to move down a slope with an incline of 10° with roller-skating gait. Roller-skating gait showed a better performance than modified walking gait in terms of mobile velocity and energy efficiency, especially moving down a slope.

Since there is a different step loss for four legs during walking, the direction of movement of the robot is unstable. For the improvement of the walking stability of the wheeled robot in longitudinal direction, we proposed a closed-loop control method by carrying a gyroscope sensor to measure the yaw angle of the robot in real time. Finally, we conducted plenty of walking experiments to evaluate a good performance of directional control.

Acknowledgment

This research is partly supported by National Natural Science Foundation of China (61375094), Key Research Program of the Natural Science Foundation of Tianjin (13JCZDJC26200), National High Tech. Research and Development Program of China (No. 2015AA043202), and SPS KAKENHI Grant Number 15K2120.

References

- [1] J. Yu, R. Ding, Q. Yang, M. Tan, J. Zhang, Amphibious pattern design of a robotic fish with wheel-propeller-fin mechanisms, *J. Field Robot.* (2013) 1–15.
- [2] A.J. Ijspeert, A. Crespi, D. Ryczko, J.M. Cabelguen, From swimming to walking with a salamander robot driven by a spinal cord model, *Science* 315 (2007) 1416–1420.
- [3] K. Tadakuma, R. Tadakuma, M. Aigo, M. Shimojo, M. Higashimori, M. Kaneko, "Omni-Paddle": Amphibious Spherical Rotary Paddle Mechanism, in: Proceedings of 2011 IEEE International Conference on Robotics and Automation

- (2011), pp. 5056–5062.
- [4] G. Dudek, P. Giguere, C. Prahacs, S. Saunderson, J. Sattar, L. Torres-Mendez, M. Jenkin, A. German, A. Hogue, A. Ripsman, J. Zacher, E. Milios, H. Liu, P. Zhang, M. Buehler, C. Georgiades, AQUA: an amphibious autonomous robot, *Computer* 40 (1) (2007) 46–53.
- [5] S. Zhang, X. Liang, L. Xu, M. Xu, Initial development of a novel amphibious robot with transformable fin-leg composite propulsion mechanisms, *J. Bionic Eng.* 10 (4) (2013) 434–445.
- [6] M. Li, S. Guo, H. Hirata, H. Ishihara, Design and performance evaluation of an amphibious spherical robot, *Robot. Auton. Syst.* 64 (2015) 21–34, <http://dx.doi.org/10.1016/j.robot.2014.11.007>.
- [7] C.P. Santos, V. Matos, Gait transition and modulation in a quadruped robot: a brainstem-like modulation approach, *Robot. Auton. Syst.* 59 (2011) 620–634.
- [8] V. Matos, C.P. Santos, Omnidirectional locomotion in a quadruped robot: A CPG-based approach, in: *IEEE/RSJ International Conference on Intelligent Robots and Systems (IROS)* (2010), pp. 3392–3397.
- [9] C.P. Santos, V. Matos, CPG modulation for navigation and omnidirectional quadruped locomotion, *Robot. Auton. Syst.* 60 (6) (2012) 912–927.
- [10] G. Endo, S. Hirose, Study on roller-walker (system integration and basic experiments), in: *Proceedings of 1999 IEEE International Conference on Robotics and Automation* (1999), pp. 2032–2037.
- [11] G. Endo, S. Hirose, Study on roller-walker (Adaptation of characteristics of the propulsion by a leg trajectory), *Intelligent Robots and Systems, IROS 2008* (2008), pp. 1532–1537.
- [12] G. Endo, S. Hirose, Study on roller-walker (energy efficiency of roller-walker), in: *Proceedings of 2011 IEEE International Conference on Robotics and Automation* (2011), pp. 5050–5055.
- [13] G. Endo, S. Hirose, Study on roller-walker (Multi-mode steering control and self-contained locomotion), in: *Proceedings of the 2000 IEEE International Conference on Robotics and Automation* (2000), pp. 2808–2814.
- [14] X. Ding, K. Xu, Design and analysis of a novel metamorphic wheel-legged rover mechanism, *J. Cent. South Univ. (S1)* (2009) S91–S101.
- [15] S. Shen, C. Li, C. Cheng, J. Lu, S. Wang, P. Lin, Design of a leg-wheel hybrid mobile platform IROS 2009, *Intell. Robot. Syst.* (2009) 4682–4687.
- [16] F. Michaud, S. Caron, Multi-modal locomotion robotic platform using leg-track-wheel articulations, *Auton. Robot.* (2005) 137–156.
- [17] S. Guo, M. Li, C. Yue, Performance evaluation on land of an amphibious spherical mother robot in different terrains, in: *Proceedings of 2013 IEEE International Conference on Mechatronics and Automation* (2013), pp.1173–1178.
- [18] S. Guo, M. Li, L. Shi, S. Mao, C. Yue, “Performance evaluation on land of an amphibious spherical mother robot”, in: *Proceedings of the 2013 ICME International Conference on Complex Medical Engineering*, Beijing, China, May 25–28 (2013), pp. 602–607.
- [19] C. Iverach-Breton, J. Baltes, J. Anderson, A. Winton, D. Carrier, Gait design for an ice skating humanoid robot, *Robot. Auton. Syst.* 62 (2014) 306–318.
- [20] M. Li, S. Guo, C. Yue, A Roller Skating Mode-based Amphibious Spherical Robot, in: *Proceedings of 2014 IEEE International Conference on Mechatronics and Automation*, Tianjin, China, , August 3–6 (2014), pp. 1957–1961.
- [21] Y. Li, S. Guo, C. Yue, Preliminary concept of a novel spherical underwater robot, *Int. J. Mechatron. Autom.* 5 (1) (2015) 11–21.
- [22] S. Zhang, Y. Zhou, M. Xu, X. Liang, J. Liu, J. Yang, AmphiHex-I: locomotory performance in amphibious environments with specially designed transformable flipper legs, *IEEE/ASME Trans. Mechatron.* 21 (3) (2016) 1720–1731.
- [23] A. Crespi, K. Karakasiliotis, A. Guignard, A.J. Ijspeert, Salamandra robotica II: an amphibious robot to study salamander-like swimming and walking gaits, *IEEE Trans. Robot.* 29 (2) (2013) 308–320.